

Integrated analysis of differentially expressed genes, differentially methylated genes, and natural compounds in hepatitis C virus-induced cirrhosis

Junxiong Cheng¹ , Zhiwei Chen¹,
Guoqing Zuo^{1,2} and Wenfu Cao¹

Abstract

Objective: To identify key genes in hepatitis C virus (HCV)-induced cirrhosis and to predict effective drugs for its treatment.

Methods: Three datasets were used to screen for differentially expressed genes (DEGs) and differentially methylated genes (DMGs) in HCV-induced cirrhosis. DEGs were subjected to Gene Ontology and Kyoto Encyclopedia of Genes and Genomes pathway enrichment analyses using the clusterProfiler R package. Their respective protein–protein interaction (PPI) networks were constructed using Cytoscape. Cross analysis of DEGs and DMGs was performed to identify the genetic landscape of HCV-induced cirrhosis, and five genes were validated by receiver operating characteristic curve analysis. Molecular autodocking between *ISG15* and natural products was performed using AutoDock Tool 1.5.6.

Results: A total of 357 DEGs and 8,830 DMGs were identified. DEG functional analysis identified several pathways involved in the pathogenesis of HCV-induced cirrhosis. Cross analysis of DEGs and DMGs identified 212 genes, and PPI network analysis identified 25 hub genes. Finally, five genes including *ISG15* were identified and confirmed in dataset GSE36411. Artesunate and betulinic acid were shown to have a strong binding affinity to *ISG15*.

²Department of Gastroenterology, Chongqing Hospital of Traditional Chinese Medicine, Chongqing, P. R. China

Corresponding author:

Guoqing Zuo, Department of Gastroenterology, Chongqing Hospital of Traditional Chinese Medicine, No. 6 Panxi Seventh Branch Road, Jiangbei District, Chongqing 400011, P. R. China.
Email: cqzqly@163.com

¹College of Traditional Chinese Medicine, Chongqing Medical University, Chongqing Key Laboratory of Traditional Chinese Medicine for Prevention and Cure of Metabolic Diseases, Chongqing, P. R. China



Conclusion: Our study provides novel insights into the mechanisms of HCV-induced cirrhosis which could lead to the identification of new therapeutics.

Keywords

Hepatitis C virus, cirrhosis, differentially expressed gene, differentially methylated gene, molecular docking, ISG15

Date received: 8 August 2021; accepted: 24 December 2021

Introduction

Cirrhosis is a chronic liver disease characterized by esophageal varices, ascites, and high portal pressure following the formation of fibrous septae and nodules; it ultimately leads to liver structure collapse.¹ Cirrhosis usually occurs after liver injury induced by viral infections, alcoholic abuse, immune dysfunction, and biliary disease.² Among these etiologies, hepatitis C virus (HCV) infection plays an important role. Although the hepatitis B virus epidemic is becoming controlled in China,³ it remains a challenge to prevent hepatitis C from progressing to cirrhosis, especially when it is caused by HCV genotype 1.⁴ Therefore, it is necessary to better understand the underlying molecular features of HCV-mediated cirrhosis for enhanced and adequate treatment.

DNA methylation is a basic biological process that plays an important role in cellular processes and organ function.⁵ DNA hypermethylation is thought to lead to the downregulation or inhibition of gene expression,⁶ but this hypothesis has been challenged.⁷ Liver fibrosis is usually accompanied by changes in methylation in the entire genome or within particular genes.^{8–10} However, the mechanisms by which genes are regulated by DNA methylation in cirrhosis remain unclear.

Bioinformatics is an emerging and rapidly developing field that relies on sequencing and information technologies to analyze

big data.¹¹ The present study investigated the combined gene expression and DNA methylation profiles of HCV-mediated cirrhosis to provide novel insights into underlying molecular mechanisms and the relationship between DNA methylation and gene expression. Two gene expression profiles (GSE6764 and GSE14323) and one methylation profile (GSE60753) obtained from the Gene Expression Omnibus (GEO) database were used to identify differentially expressed genes (DEGs) and differentially methylated CpG sites and genes, respectively. Potential associations between the DEGs was investigated by constructing protein–protein interaction (PPI) networks, and the potential pathological role of key genes was further validated with an independent cohort (GSE36411).

Materials and methods

Access of GSE datasets

The terms “HCV” and “cirrhosis” or “liver fibrosis” were used to retrieve valuable datasets from the GEO database with the following inclusion criteria: 1) including at least two groups (control and HCV-mediated cirrhosis), and 2) a sample size >20. Two expression datasets (GSE6764 and GSE14323) were included in the study (Table 1). Ethical approval was not applicable for the present study because no

Table 1. Dataset used for analysis.

GEO ID	Platform	Control	HCV-mediated cirrhosis
GSE14323	GPL571	19	41
GSE6764	GPL570	10	13
GSE60753	GPL13534	33	38
GSE36411	GPL10558	21	21

patients were recruited and no animal work was carried out.

Identification of DEGs

R packages (www.r-project.org) *limma* and *preprocessCore* were used to perform background correction and quantile normalization, respectively. Each probe name was converted into gene symbols according to GPL570 and GPL96 annotation files. The *limma* R package was further used to identify DEGs between HCV-mediated cirrhosis and control samples. A false discovery rate < 0.05 , adjusted p -value < 0.05 , and $|\log_2 \text{fold change}| > 1$ were considered cutoff values for DEG screening.

Functional enrichment analysis of DEGs

Gene ontology (GO) and Kyoto Encyclopedia of Genes and Genomes (KEGG) signaling pathway enrichment analyses were performed of the identified DEGs using the *clusterProfiler* R package. Key pathways or processes with $p < 0.05$ and a gene number ≥ 5 were recognized.

Methylation analysis of cirrhosis

The GEO dataset GSE60753 containing DNA methylation profiles of the liver was analyzed using the *ChAMP* R package. After quality control, two samples (GSM1487212 and GSM1487117) were discarded (Table 1). Thus, 34 control samples and 39 samples from patients with HCV-mediated cirrhosis were included in the analysis.

Differentially methylated probes (DMPs) were defined as cytosine–phosphate–guanine (CpG) sites with $|\Delta\text{Beta}| \geq 0.1$ and adjusted $p < 0.05$. Genes displaying at least one DMP were identified as differentially methylated genes (DMGs).

Cross-analysis of DEGs and DMGs

To explore the effect of DNA methylation on gene expression in HCV-mediated cirrhosis, all DEGs with methylation changes were identified and the regions of methylation in these genes were analyzed.

Construction of PPI network

All DEGs were submitted to the STRING database (<http://string-db.org>) prior to being filtered into the defined PPI network and modified using the Cytoscape platform (v3.6.0). Then, the maximal clique centrality method (MCC) in the plugin cytoHubba was used to identify hub genes, with a score $> 1 \times 10^{11}$ considered significant.

Receiver operator characteristic (ROC) curve analysis of methylated hub genes

The whole methylation status of 25 hub genes was analyzed based on previously identified DMPs. The expression of genes with a DNA methylation change was evaluated in the GSE14323 dataset by ROC curve analysis, with $p < 0.05$ considered statistically significant and the genes considered relevant to HCV-mediated cirrhosis.

Validation of key genes

To further validate the study findings, GEO dataset GSE36411 (containing information on 21 HCV-mediated cirrhosis and 21 control samples) was used to confirm the expression of hub genes. Expression comparisons were performed by a Student's t -test in GraphPad Prism 8.0 (GraphPad

Software, San Diego, CA, USA), with $p < 0.05$ considered statistically significant.

Molecular docking

To explore compounds that might target key genes, we downloaded the structure of 31 small molecules targeting liver cirrhosis in pdb format¹² from PubChem (<https://pubchem.ncbi.nlm.nih.gov/>), as well as the crystal structure of ISG15 (1Z2M) from RCSB PDB (<https://www1.rcsb.org/>). Molecular docking was performed using Auto Dock Tools 1.5.6 and a rigid docking protocol that used a genetic algorithm to generate binding poses of the

protein–ligand complexes. The first binding energy of each complex was recorded.

Results

Identification of DEGs in HCV-cirrhosis

A total of 856 and 273 genes were found to be upregulated and downregulated, respectively, in HCV-mediated cirrhosis samples compared with controls in the GSE6764 dataset, in addition to 737 upregulated and 10 downregulated genes in the GSE14323 dataset (Figures 1 and 2). In total, 357 genes (350 upregulated and 7 downregulated) that were differentially expressed in HCV-mediated cirrhosis

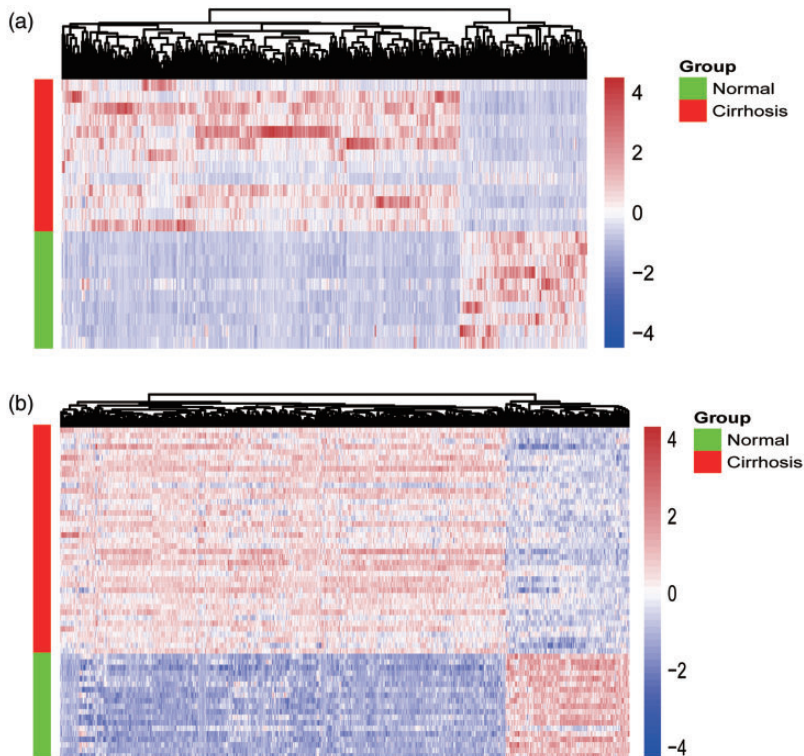


Figure 1. Heatmap of DEGs in HCV-mediated cirrhosis. All DEGs identified in (a) GSE6764 and (b) GSE14323 datasets are shown.

DEGs, differentially expressed genes; HCV, hepatitis C virus.

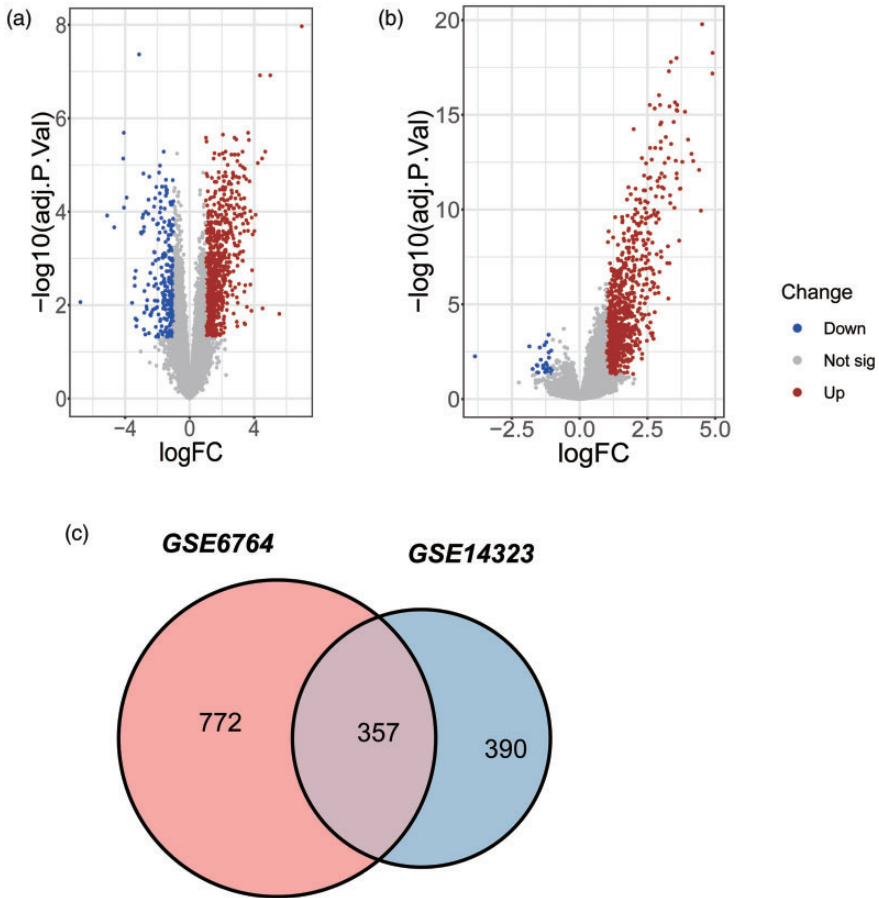


Figure 2. Volcano plots and Venn diagrams of DEGs. Each point in the volcano map represents a gene. Red, blue, and gray represent upregulated, downregulated, and non-significantly changed genes, respectively in (a) GSE6764 and (b) GSE14323 datasets. DEGs, differentially expressed genes.

samples compared with controls in both datasets were identified as DEGs (Table 2).

Functional enrichment analysis of DEGs

To explore the function of the identified DEGs, GO and KEGG analyses were performed. The top eight significant GO and KEGG pathways are shown in Figure 3. Overall, extracellular matrix structural constituent, extracellular matrix organization, collagen-containing extracellular matrix, and focal adhesion were the most

significant functions or pathways identified pertaining to molecular function, biological processes, and cellular component, as well as KEGG terms. Response to virus was also identified as a significant biological process, and influenza A as a significant pathway in KEGG analysis.

Identification of DMGs in HCV-mediated cirrhosis

A total of 25,125 CpG sites were identified as DMPs and 8830 genes identified as

Table 2. Differentially expressed genes identified in the two datasets.

Differentially expressed genes	
Upregulated	ZNF83, WIPF1, VWF, VIM, VEGFC, VCAN, TYMS, TUSC3, TRIM22, TRBC1, TRAC, TPSB2, TPSAB1, TPM2, TPM1, TNFRSF21, TNFAIP8, TNFAIP2, TMPRSS3, TMEM30B, TMEM100, THY1, THSD7A, THEMIS2, THBS2, TGFBI, TESC, TCF4, TAGLN, TACSTD2, SWAP70, SVEP1, STON, STMN2, STK39, STC1, STAT1, SPPI, SPON1, SPOCK2, SPINT2, SPI10, SPI00, SOX9, SOX4, SLIT2, SLC25A36, SLC25A24, SLC1A3, SLAMF8, SINHCAF, SH3YL1, SFRP5, SERPINB9, SEPTIN6, SELIL3, SCRNI, S100A6, S100A14, S100A11, RUNX3, RTP4, ROBO1, RNASET2, RNASE6, RNASE1, RGS4, RGS10, RGS1, RFX5, RBP1, RASGRP1, RAI2, RAC2, RAB25, RAB11FIP1, PTPRN2, PTPRC, PTPN13, PTGIS, PTGDS, PSMB9, PROM1, PRKCB, POU2AF1, PODXL, PMP22, PLXDC2, PLVAP, PLAT, PLAGL1, PLA2G5, PLA2G4C, PIK3R3, PIK3IP1, PFKM, PECAM1, PDZK1IP1, PDLIM3, PDGFRA, PDGFRD, PDGFA, PDE4D, PDE1A, PBX1, PARP8, OASL, OAS3, OAS2, OAS1, NIBAN1, NFASC, NEDD9, NEDD4L, NCK2, NAV3, MZB1, MYOF, MYL9, MYH4, MXRA7, MX2, MX1, MUC13, MS4A4A, MOXD1, MMP7, MMP2, MLLT11, MID1, MICALL2, MGP, MFAP4, METTL9, MCUB, MCTP1, MARCKS, MACROH2A1, LYZ, LY96, LY75, LXN, LUM, LTBP2, LTB, LRRC17, LOXLI, LIF, LGALS4, LGALS3BP, LGALS3, LEF1, LDHB, LCP2, LCK, LBH, LAMC3, LAMC1, LAMB1, LAMA2, KRT7, KRT23, KRT19, KCTD12, KCNJ16, JCHAIN, JAG1, ITM2A, ITK, ITGBL1, ISG15, ISG15, IL7R, IL18, IGLV1-44, IGLL3P, IGLJ3, IGLC1, IGKC, IGK, IGHM, IGHG1, IGHD, IGFBP7, IFIT1, IFIH1, IFI6, IFI44L, IFI44, IFI35, IFI27, IFI16, ID4, ID3, HTR2B, HSPB8, HSPA2, HLA-F, HLA-DRB6, HLA-DRA, HLA-DQB1, HLA-DPBI, HLA-DPA1, HLA-DMA, HERC6, HERC5, HDGFL3, GZMK, GZMA, GUSBP11, GSTP1, GSN, GPRC5B, GPR183, GPR171, GPNMB, GPC4, GPC3, GOLM1, GMNN, GM2A, GLS, GLIPR1, GEM, GDF15, GATA6, GAS1, GABRP, FZD7, FXYD5, FXYD2, FSTL3, FRZB, FMOD, FLNA, FLII, FGFR2, FBNI, FBLN5, FBLN1, FAP, FAIM, F3, EZR, EVI2B, EVI2A, EPHA3, EPCAM, ENPP2, ENDOD1, EMP3, EFEMP2, EFEMPI, DPYSL3, DPT, DKK3, DEPPI, DEFB1, DDX60, DCN, CYTIP, CYTH2, CYBRD1, CYBA, CXCR4, CXCL9, CXCL6, CXCL10, CXCL1, CTSK, CTBP2, CRISPLD2, CRIP2, CRIP1, CRIM1, CPE, CPA3, CORO1A, COL6A3, COL5A1, COL4A3, COL4A2, COL4A1, COL3A1, COL1A2, COL1A1, COL15A1, COL14A1, CLSTN1, CLECI1A, CLDN10, CHST4, CHRDL1, CH25H, CFTR, CELF2, CDKN1C, CDH11, CDC42EP3, CD8A, CD74, CD69, CD53, CD52, CD48, CD44, CD37, CD24, CD2, CCR7, CCND2, CCN2, CCL5, CCL21, CCL20, CCL19, CAVINI, CASP1, CALD1, C7, BTN3A3, BST2, BICCI, BCL2, BATE, BACE2, ARL4C, ARHGEF3, AQPI, APOL3, APOBEC3G, ANXA3, ANXA13, ANXA1, ANKRD36B, ANKRD36B, ANK3, ANK2, ALOX5AP, ALOX5, AKR1B10, AKR1B1, AEBP1, ADGRG2, ADGRA2, ADAMTSL2, ADA2, ACSL4, ACKR3, ABCC4
Downregulated	ALPL, SLC04C1, DHRS2, PCOLCE2, KCNN2, GYG2, MME

DMGs. Of these, 3831 genes had only one DMP, whereas the others had at least two DMPs.

Cross analysis of DMGs and DEGs identified 212 genes (Figure 4 and Supplementary Table 1), of which 131 genes were upregulated and hypermethylated, 77 were upregulated and

hypomethylated, two were downregulated and hypermethylated, and two were downregulated and hypomethylated in HCV-mediated cirrhosis samples compared with controls. Almost half of the DMPs were located in the gene body (12,777), whereas only 4365 CpG methylation events occurred.

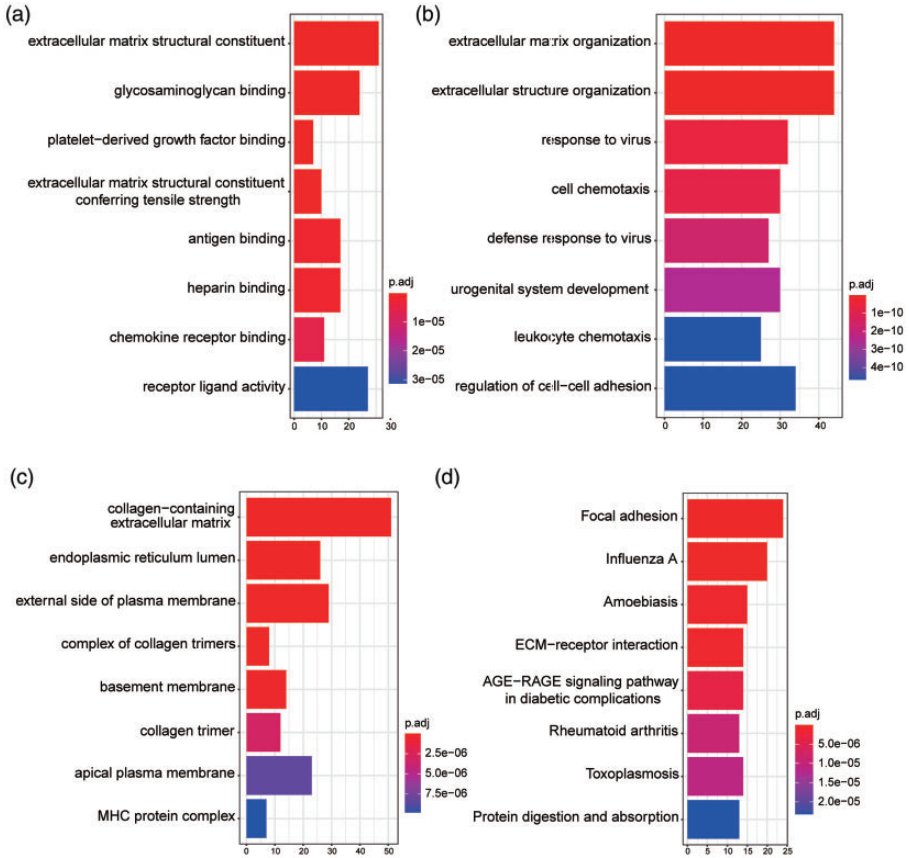


Figure 3. Top eight significantly enriched GO terms and KEGG pathways of DEGs in HCV-mediated cirrhosis. (a) Molecular function. (b) Biological process. (c) Cellular component. (d) KEGG pathways. x axis shows the frequency of each term; y axis indicates GO terms or KEGG pathways; colors represent adjusted p-values.

DEGs, differentially expressed genes; GO, gene ontology; HCV, hepatitis C virus; KEGG, Kyoto Encyclopedia of Genes and Genomes.

PPI network construction and hub genes identification

To better understand which of the shared DEGs were most likely to be key genes in the development of HCV-mediated cirrhosis, a PPI network of 357 DEGs was constructed (Supplementary Figure 1). Fifty-four genes were excluded from this network while 303 were included. A total of 303 nodes and 1932 edges were displayed. According to the MCC method in CytoHubba, 25 genes (*OASL*, *OAS1*,

OAS2, *MX1*, *OAS3*, *ISG15*, *IFIT1*, *TRIM22*, *MX2*, *IFI35*, *IFI6*, *STAT1*, *IFIH1*, *IFI44L*, *IFI44*, *BST2*, *IFI27*, *CXCL10*, *HERC6*, *RTP4*, *HERC5*, *DDX60*, *ISG20*, *IFI16*, and *SP110*) were deemed hub genes, suggesting that they are likely to be essential for fibrogenesis in patients with HCV (Figure 5).

Methylation status of the hub genes

Next, changes in the methylation status among the 25 hub genes were analyzed.

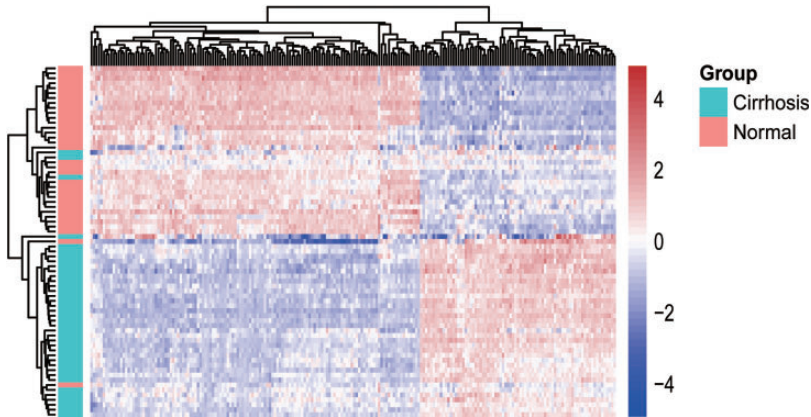


Figure 4. DMGs in the GSE60753 dataset. Heatmap of the top 212 DMGs and DEGs. DMG, differentially methylated genes; DEGs, differentially expressed genes.

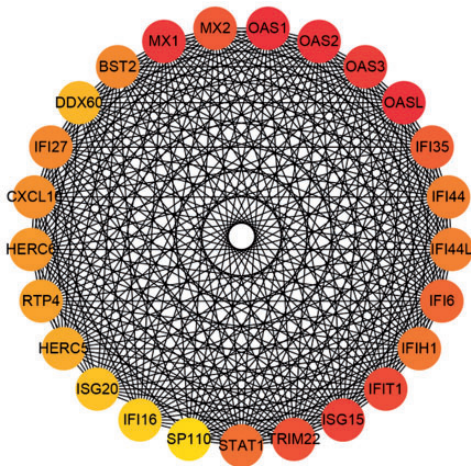


Figure 5. Network of the top 25 hub genes identified in HCV-mediated cirrhosis. A redder color represents a higher score in Cytoscape based on the MCC method. HCV, hepatitis C virus; MCC, maximal clique centrality.

Overall, 11 genes (*OASL*, *OAS3*, *IFI35*, *IFI6*, *IFIH1*, *IFI44*, *CXCL10*, *HERC6*, *RTP4*, *HERC5*, and *SP110*) displayed no significant methylation changes, whereas the other 14 hub genes were hypermethylated, showing significant changes in at least one CpG site (Supplementary Table 2).

ROC curve analysis

The performance of the 14 differentially methylated hub genes as diagnostic biomarkers was examined by ROC curve analyses. *ISG15* (area under the curve [AUC] = 0.9987 [0.9945–1.000, $p < 0.0001$]), *TRIM22* (AUC = 0.9974 [0.9906–1.000, $p < 0.0001$]), *IFI44L* (AUC = 0.9961 [0.9868–1.000, $p < 0.0001$]), *IFI27* (AUC = 1 [1.000–1.000, $p < 0.0001$]), and *IFI16* (AUC = 0.9936 [0.9794–1.000, $p < 0.0001$]) were identified as potential markers (Figure 6).

Validation of hub genes

The expression of *ISG15*, *TRIM22*, *IFI44L*, *IFI27*, and *IFI16* was next determined in GSE36411, and that of *ISG15*, *TRIM22*, *IFI27*, and *IFI16* shown to be significantly higher in patients with HCV-mediated cirrhosis compared with controls ($p < 0.001$; Figure 7).

Binding results

Compounds with the highest binding affinities for *ISG15* were artesunate (–6.27 kcal/mol) and betulinic acid (–6.23 kcal/mol) (Supplementary Figure 2). Detailed information including numbers of hydrogen

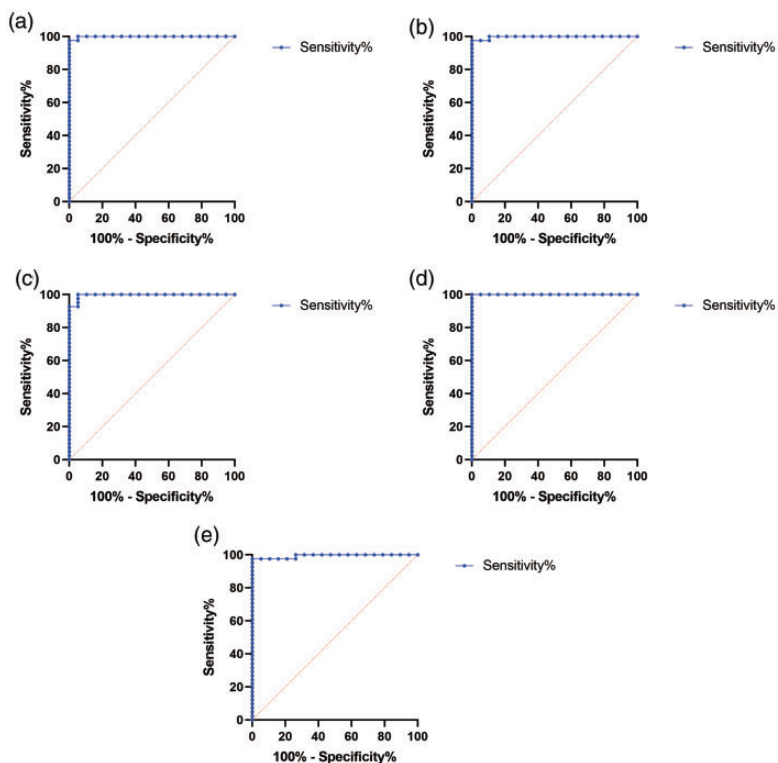


Figure 6. ROC curves of *ISG15* (a), *TRIM22* (b), *IFI44L* (c), *IFI27* (d), and *IFI16* (e) for an HCV-mediated cirrhosis diagnosis.

HCV, hepatitis C virus; ROC, receiver operator characteristic.

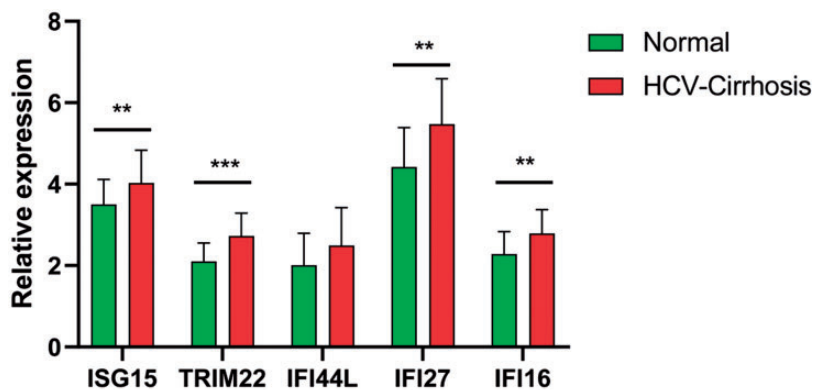


Figure 7. Validation of *ISG15*, *TRIM22*, *IFI44L*, *IFI27*, and *IFI16* differential expression in the GSE36411 dataset. ** $p < 0.01$, *** $p < 0.001$ using a Student's t -test comparison.

Table 3. Binding energy of 31 small molecule drugs showing affinity to ISG15.

Drug	Pubchem ID	Formula	Molecular weight	Binding energy (kcal/mol)	Hydrogen bond
Berberine	2353	C ₂₀ H ₁₈ NO ₄ ⁺	336.4	-5.57	1
Caffeine	2519	C ₈ H ₁₀ N ₄ O ₂	194.19	-4.27	1
Capsaicin	1548943	C ₁₈ H ₂₇ NO ₃	305.4	-4.44	1
Evodiamine	442088	C ₁₉ H ₁₇ N ₃ O	303.4	-5.81	1
Ligustrazine	14296	C ₈ H ₁₂ N ₂	136.19	-3.97	1
Matrine	91466	C ₁₅ H ₂₄ N ₂ O	248.36	-5.6	1
Melatonin	896	C ₁₃ H ₁₆ N ₂ O ₂	232.28	-4.44	2
Neferine	159654	C ₃₈ H ₄₄ N ₂ O ₆	624.8	-2.94	2
Oxymatrine	114850	C ₁₅ H ₂₄ N ₂ O ₂	264.36	-5.39	1
Tetrandrine	73078	C ₃₈ H ₄₂ N ₂ O ₆	622.7	-3.96	0
Apigenin	5280443	C ₁₅ H ₁₀ O ₅	270.24	-5.16	3
Baicalin	64982	C ₂₁ H ₁₈ O ₁₁	446.4	-3.32	3
Breviscapine	6426802	C ₂₁ H ₁₈ O ₁₂	462.4	-5.27	1
Chrysin	5281607	C ₁₅ H ₁₀ O ₄	254.24	-5.92	3
Diosmin	5281613	C ₂₈ H ₃₂ O ₁₅	608.5	-2.7	3
Hesperetin	72281	C ₁₆ H ₁₄ O ₆	302.28	-5.4	1
Hyperoside	5281643	C ₂₁ H ₂₀ O ₁₂	464.4	-4.88	3
Icaritin	5318980	C ₂₁ H ₂₀ O ₆	368.4	-4.87	1
Morin	5281670	C ₁₅ H ₁₀ O ₇	302.23	-4.58	1
Myricetin	5281672	C ₁₅ H ₁₀ O ₈	318.23	-4.22	3
Naringenin	932	C ₁₅ H ₁₂ O ₅	272.25	-5.41	2
Oroxylin A	5320315	C ₁₆ H ₁₂ O ₅	284.26	-4.87	2
Proanthocyanidin	108065	C ₃₁ H ₂₈ O ₁₂	592.5	-3.35	4
Puerarin	5281807	C ₂₁ H ₂₀ O ₉	416.4	-4.51	3
Silibinin	31553	C ₂₅ H ₂₂ O ₁₀	482.4	-4.6	1
Wogonoside	3084961	C ₂₂ H ₂₀ O ₁₁	460.4	-3.8	2
Artesunate	6917864	C ₁₉ H ₂₈ O ₈	384.4	-6.27	1
Betulinic acid	64971	C ₃₀ H ₄₈ O ₃	456.7	-6.23	2
Paoniflorin	442534	C ₂₃ H ₂₈ O ₁₁	480.5	-2.31	1
Curcumin	969516	C ₂₁ H ₂₀ O ₆	368.4	-4.15	3
Resveratrol	445154	C ₁₄ H ₁₂ O ₃	228.24	-4.95	1

bonds formed between ISG15 and small molecules is listed in Table 3.

Discussion

Treatment approaches to cirrhosis are limited, in part because disease progression is not fully understood. In the present study, cross analysis of HCV-mediated cirrhosis genetic and epigenetic profiles was performed with the aim of improving our understanding of HCV-mediated cirrhosis.

In total, 357 DEGs were identified, including the fibrosis initiation factor transforming growth factor (TGF)- β , *PDGFA*, and *PDGFD*, which are critical to the activation of hepatic stellate cells (HSCs).^{13,14} Moreover, the expression of collagen deposition-related genes, including *COL1A1*, *COL1A2*, *COL4A1*, *COL4A2*, and *COL4A3*, was increased in HCV-mediated cirrhosis samples. Other important genes, such as *STAT1*, and the *CXCL* family, which is associated with cirrhosis, also showed increased expression.

GO enrichment analysis of DEGs demonstrated that their molecular function was mainly enriched in extracellular matrix structural constituent, glycosaminoglycan binding, and receptor ligand activity, while their biological function was mainly enriched in extracellular matrix organization, extracellular structure organization, response to virus, defense response to virus, and the regulation of cell–cell adhesion. Moreover, cellular components were mainly enriched in collagen-containing extracellular matrix, endoplasmic reticulum lumen, and the external side of the plasma membrane. This suggests that extracellular matrix deposition is a basic pathological change in cirrhosis. The response to virus was also enriched in identified DEGs, and previous research found that the response to HCV causes chronic inflammation, which is a vital activator of myofibroblast transdifferentiation.¹⁵ HCV infection not only destroys hepatocytes, but also induces the expression of TGF- β family members.¹⁶ Therefore, antivirals are the principal therapeutic approach for HCV-mediated cirrhosis.¹⁷ A previous study found that cirrhosis is reversible when its etiological factors are abolished,¹⁸ further indicating the importance of TGF- β in cirrhosis.

KEGG analysis of DEGs in this study revealed that the main pathways involved in HCV-mediated cirrhosis are focal adhesion, influenza A, the extracellular matrix–receptor interaction, protein digestion, and absorption. Focal adhesion kinase, a member of the tyrosine kinase superfamily, was previously found to regulate the activation of HSCs and liver fibrosis.¹⁹ Phosphoinositide 3-kinase (PI3K) is a member of the focal adhesion pathway, and the PI3K/AKT/mammalian target of rapamycin pathway induces autophagy during HSC activation, thereby leading to fibrosis.²⁰ Furthermore, identified DEGs within the advanced glycation endproducts (AGE)/receptor for AGE signaling

pathway, including TGF- β 1, BCL2, STAT1, and MMP2, were also associated with cirrhosis.²¹ Moreover, VEGFC was found to be beneficial for cirrhotic rats with hepatic encephalopathy,²² but the detailed mechanisms require further investigations.

DNA methylation is a key event in cellular and molecular biological processes. Although past studies have documented reduced methylation levels in CCL₄-induced liver fibrosis,¹⁰ controversial findings regarding the hypermethylation of particular genes that are upregulated in fibrosis models have been reported.²³ For example, longer CCL₄ exposure was shown not to significantly alter the DNA methylation status.²⁴ In turn, the methylation of promoters of several genes, such as P14, P15, P73, and MGMT, was increased in liver disease including cirrhosis.²⁵

The diversity of the DNA methylation status in cirrhosis is undeniable. Indeed, gene expression might not negatively correlate with methylation levels as they could increase the binding affinity of corresponding transcription factors.²⁶ Although methylation at CpG islands of transcription start sites (TSSs) represses gene expression, its effect on non-CpG island TSSs is unknown.²⁷ Our present results indicate that not all DEGs were hyper- or hypomethylated. Of the 25 hub genes, 11 showed no methylation changes and 6 were hypermethylated at only one CpG site, whereas the others were hypermethylated at more than one site. Thus, it is difficult to judge the impact of DNA methylation on the expression of genes that are methylated at different sites/levels. More detailed studies are needed to clarify the underlying mechanisms.

Of the 25 hub genes identified in this study, including OAS, MX, IFI, and HERC family members, OAS1 and MX1 polymorphisms were previously found to be associated with the severity of liver disease in patients co-infected with the human

immunodeficiency virus and HCV.^{28,29} Moreover, *MX1* is upregulated in activated HSCs.³⁰ Thus, it is reasonable to speculate that *MX1* promotes HSC activation and is related to the prognosis of HCV-mediated cirrhosis, although this hypothesis should be verified. Moreover, while *OAS1* and *IFI44* expression was increased in patients with systemic sclerosis-related interstitial lung disease, their function in cirrhosis has not been addressed. Of the five identified biomarkers, *IFI27* and *ISG15* were previously shown to be significantly increased in patients with non-sustained virological response (SVR) compared with patients with SVR;³¹ in contrast, the functions of *TRIM22*, *IFI44L*, and *IFI16* require further investigation. Although *OAS1* and *MX1* could be epigenetic biomarkers of HCV-mediated cirrhosis, their function should be further investigated.

The observed binding energy of natural compounds artesunate and betulinic acid for *ISG15* indicates their promising anti-fibrotic effects. Notably, both have shown anti-fibrotic effects in rat models of liver fibrosis.^{32,33} Thus, we speculate that *ISG15* is a promising therapeutic target for HCV-induced liver fibrosis.

Conclusion

Herein, DEGs in cirrhosis were identified, along with their related pathways which include focal adhesion, influenza A, and protein digestion and absorption. Furthermore, the effect of DNA methylation on gene expression in cirrhosis was explored, but this warrants further detailed assessment. Last, *OAS1* and *MX1* were identified as potential targets of HCV-mediated cirrhosis.

Author contributions

Wenfu Cao and Guoqing Zuo conceived and designed the study. Junxiong Cheng and Zhiwei Chen performed the data analysis.

Junxiong Cheng wrote the manuscript. All authors were responsible for reviewing data. All authors read and approved the final manuscript.

Declaration of conflicting interest

The authors declare that there is no conflict of interest.

Funding

The authors disclosed receipt of the following financial support for the research, authorship, and/or publication of this article: This work was funded by the National Natural Science Foundation of China (Grant No: 81573860).

ORCID iD

Junxiong Cheng  <https://orcid.org/0000-0001-7998-5938>

Supplemental material

Supplemental material for this article is available online.

References

1. Parola M and Pinzani M. Liver fibrosis: Pathophysiology, pathogenetic targets and clinical issues. *Mol Aspects Med* 2019; 65: 37–55.
2. Zhang CY, Yuan WG, He P, et al. Liver fibrosis and hepatic stellate cells: Etiology, pathological hallmarks and therapeutic targets. *World J Gastroenterol* 2016; 22: 10512–10522.
3. Scaglione S, Kliethermes S, Cao G, et al. The epidemiology of cirrhosis in the United States: A population-based study. *J Clin Gastroenterol* 2015; 49: 690–696.
4. Kohli A, Shaffer A, Sherman A, et al. Treatment of hepatitis C: a systematic review. *JAMA* 2014; 312: 631–640.
5. Moore LD, Le T and Fan G. DNA methylation and its basic function. *Neuropsychopharmacology* 2013; 38: 23–38.
6. Borowa-Mazgaj B, De Conti A, Tryndyak V, et al. Gene expression and DNA methylation alterations in the glycine N-methyltransferase gene in diet-induced

- nonalcoholic fatty liver disease-associated carcinogenesis. *Toxicol Sci* 2019; 170: 273–282.
7. Ding Z, Qian YB, Zhu LX, et al. Promoter methylation and mRNA expression of DKK-3 and WIF-1 in hepatocellular carcinoma. *World J Gastroenterol* 2009; 15: 2595–2601.
 8. Wilson CL, Mann DA and Borthwick LA. Epigenetic reprogramming in liver fibrosis and cancer. *Adv Drug Deliv Rev* 2017; 121: 124–132.
 9. Bian EB, Zhao B, Huang C, et al. New advances of DNA methylation in liver fibrosis, with special emphasis on the crosstalk between microRNAs and DNA methylation machinery. *Cell Signal* 2013; 25: 1837–1844.
 10. Komatsu Y, Waku T, Iwasaki N, et al. Global analysis of DNA methylation in early-stage liver fibrosis. *BMC Med Genomics* 2012; 5: 5.
 11. Gauthier J, Vincent AT, Charette SJ, et al. A brief history of bioinformatics. *Brief Bioinform* 2019; 20: 1981–1996.
 12. Shan L, Liu Z, Ci L, et al. Research progress on the anti-hepatic fibrosis action and mechanism of natural products. *Int Immunopharmacol* 2019; 75: 105765.
 13. Dewidar B, Meyer C, Dooley S, et al. TGF- β in hepatic stellate cell activation and liver fibrogenesis—updated 2019. *Cells* 2019; 8: 1419.
 14. Borkham-Kamphorst E, Meurer SK, Van De Leur E, et al. PDGF-D signaling in portal myofibroblasts and hepatic stellate cells proves identical to PDGF-B via both PDGF receptor type alpha and beta. *Cell Signal* 2015; 27: 1305–1314.
 15. Irshad M, Gupta P and Irshad K. Immunopathogenesis of liver injury during hepatitis C virus infection. *Viral Immunol* 2019; 32: 112–120.
 16. Chida T, Ito M, Nakashima K, et al. Critical role of CREBH-mediated induction of transforming growth factor beta2 by hepatitis C virus infection in fibrogenic responses in hepatic stellate cells. *Hepatology* 2017; 66: 1430–1443.
 17. Roehlen N, Crouchet E and Baumert TF. Liver fibrosis: mechanistic concepts and therapeutic perspectives. *Cells* 2020; 9: 875.
 18. Sun M and Kisseleva T. Reversibility of liver fibrosis. *Clin Res Hepatol Gastroenterol* 2015; 39: S60–S63.
 19. Zhao XK, Yu L, Cheng ML, et al. Focal adhesion kinase regulates hepatic stellate cell activation and liver fibrosis. *Sci Rep* 2017; 7: 4032.
 20. Wang H, Liu Y, Wang D, et al. The upstream pathway of mTOR-mediated autophagy in liver diseases. *Cells* 2019; 8: 1597.
 21. Martí-Rodrigo A, Alegre F, Moragrega ÁB, et al. Rilpivirine attenuates liver fibrosis through selective STAT1-mediated apoptosis in hepatic stellate cells. *Gut* 2020; 69: 920–932.
 22. Hsu SJ, Zhang C, Jeong J, et al. Enhanced meningeal lymphatic drainage ameliorates neuroinflammation and hepatic encephalopathy in cirrhotic rats. *Gastroenterology* 2021; 160: 1315–1329.e13.
 23. Wu P, Huang R, Xiong YL, et al. Protective effects of curcumin against liver fibrosis through modulating DNA methylation. *Chin J Nat Med* 2016; 14: 255–264.
 24. Page A, Paoli P, Moran Salvador E, et al. Hepatic stellate cell transdifferentiation involves genome-wide remodeling of the DNA methylation landscape. *J Hepatol* 2016; 64: 661–673.
 25. Zekri AR, Nassar AA, El-Din El-Rouby MN, et al. Disease progression from chronic hepatitis C to cirrhosis and hepatocellular carcinoma is associated with increasing DNA promoter methylation. *Asian Pac J Cancer Prev* 2014; 14: 6721–6726.
 26. Yin Y, Morgunova E, Jolma A, et al. Impact of cytosine methylation on DNA binding specificities of human transcription factors. *Science* 2017; 356: eaaj2239.
 27. Jones PA. Functions of DNA methylation: islands, start sites, gene bodies and beyond. *Nat Rev Genet* 2012; 13: 484–492.
 28. Bader El Din NG, Anany MA, Dawood RM, et al. Impact of OAS1 exon 7 rs10774671 genetic variation on liver fibrosis progression in Egyptian HCV genotype 4 patients. *Viral Immunol* 2015; 28: 509–516.
 29. Garcia-Alvarez M, Berenguer J, Jimenez-Sousa MA, et al. Mx1, OAS1 and OAS2 polymorphisms are associated with the

- severity of liver disease in HIV/HCV-coinfected patients: A cross-sectional study. *Sci Rep* 2017; 7: 41516.
30. Zhong Y, Sun XX, Zhang P, et al. Identification and localization of xylose-binding proteins as potential biomarkers for liver fibrosis/cirrhosis. *Mol Biosyst* 2016; 12: 598–605.
 31. Domagalski K, Pawlowska M, Kozielwicz D, et al. The impact of IL28B genotype and liver fibrosis on the hepatic expression of IP10, IFI27, ISG15, and MX1 and their association with treatment outcomes in patients with chronic hepatitis C. *PLoS One* 2015; 10: e0130899.
 32. Lai L, Chen Y, Tian X, et al. Artesunate alleviates hepatic fibrosis induced by multiple pathogenic factors and inflammation through the inhibition of LPS/TLR4/NF-kappaB signaling pathway in rats. *Eur J Pharmacol* 2015; 765: 234–241.
 33. Wan Y, Wu YL, Lian LH, et al. The anti-fibrotic effect of betulinic acid is mediated through the inhibition of NF-kappaB nuclear protein translocation. *Chem Biol Interact* 2012; 195: 215–223.